



Original Paper

Adsorption-desorption of lead by polycarboxylate-coated bentonite

Chuang Yu^{1,2}, Zhi-lei Zeng¹ , Xiaoqing Cai³, Zhi-hao Chen¹ and Rao-ping Liao¹ 

¹College of Civil Engineering and Architecture, Wenzhou University, Wenzhou, China; ²College of Environmental Protection, Zhejiang Industry and Trade Vocational College, Wenzhou, China and ³College of Chemistry & Materials Engineering, Wenzhou University, Wenzhou, China

Abstract

To develop more economical and efficient heavy metal adsorbents, natural bentonite was employed as a raw material, and triethoxyvinylsilane served as a grafting agent to achieve the grafting bonding of sodium polyacrylate and bentonite. Structural alterations in the modified bentonite were analyzed through thermogravimetric analysis (TGA), scanning electron microscopy (SEM), and X-ray diffraction (XRD). The adsorption and desorption characteristics of SAPAS-Bentonite and raw bentonite were compared and tested under various conditions, including time, temperature, pH, and lead ion concentration. The adsorption and desorption properties of sodium polyacrylate-grafted bentonite (SAPAS-Bentonite) were compared under various conditions (time, temperature, pH, and lead ion concentration). The results revealed that the modified method successfully achieved nano-scale coating of bentonite particles with sodium polyacrylate, leading to an increase in the maximum adsorption capacity of lead ions by 47.5%, reaching 165.73 mg/g. A greater adsorption affinity for lead ions was exhibited by the outer sodium polycarboxylate portion of SAPAS-Bentonite compared with the inner bentonite. The adsorption of internal bentonite was limited by blocking when the adsorption of sodium polyacrylate did not reach the upper limit. The adsorption isotherm shifted from the Langmuir monolayer characteristic of the original bentonite to the S-shaped isotherm, reflecting the sodium polycarboxylate properties of SAPAS-Bentonite. Both bentonites demonstrated strong retention capacity for lead, with SAPAS-Bentonite surpassing raw bentonite in performance. This study provides valuable insights into the potential of SAPAS-Bentonite in the treatment of heavy metal pollution.

Keywords: Desorption; grafting; modification; polyacrylate; sorption; silane coupling agent

(Received: 21 January 2024; accepted: 22 January 2024)

Introduction

The detrimental impact of soil and water pollution, originating from industrial waste water, contaminated sites, tailings, and farmland, has become a focal point of global concern. Heavy metals, in contrast to organic pollutants, are not subject to decomposition and have a propensity for migration and dispersion through groundwater. This process culminates in the accumulation of these metals in the human body, giving rise to severe endemic diseases (Ji et al., 2013; Bai and Zhao, 2020; Kharazi et al., 2021). Consequently, strategies for the extraction and stabilization of heavy metal pollutants from water and soil are critical for the safeguarding of ecosystem security (Järup, 2003).

In response to the growing concern about heavy metal pollution, a variety of potential remediation technologies have been developed (Chai et al., 2021). These include *in situ* soil remediation methods such as biological treatment (Farrell and Jones, 2009), stabilization/solidification (Xu et al., 2021), aqueous flushing (Atteia et al., 2013), and permeable reactive barrier (Faisal et al., 2018). Additionally, liquid phase remediation technologies for industrial effluents and polluted watercourses (Kurniawan et al., 2006; Xu et al., 2022), encompass ion exchange (Dąbrowski et al., 2004), membrane

separation (Abdullah et al., 2019), adsorption (Han et al., 2019), flocculation and biological treatment (Chipasa, 2003). However, despite the strides made in technological innovation, these methods have revealed limitations in practical applications. Notably, biological treatment is constrained by the depth of contaminated soil, as it exclusively accumulates heavy metals in shallow soil through plants or bacteria. Stabilization/solidification methods, while effective in preventing the migration of heavy metals or inhibiting their activity (toxicity) through repair materials (stabilizers), grapple with the persistence of metals in the soil. The potential re-release of metals when the repair agent fails and soil salinization with the application of alkaline stabilizers like cement and lime. The aqueous flushing method, designed to remove contaminants from contaminated soil through injection-pumping, necessitates the subsequent centralized treatment of the rinsed liquid by efficient adsorbents to capture heavy metals. The permeable reactive barrier, a widely employed engineering technique, mandates coordination measures to impede the outward diffusion of contaminants on the site. This technique is commonly integrated with adsorption-reaction materials to effectively capture or stabilize contaminants. Even the membrane separation method depends on adsorbents after forming a side concentrate. Consequently, the utilization of chemical or physical adsorption for the efficient removal of contaminants presents a promising solution in the realm of soil-water pollution treatment.

Recent studies highlight activated carbon (Deliyanni et al., 2015), natural or modified biochar (Tan et al., 2015; Wang et al., 2019), and

Corresponding author: Rao-ping Liao; Email: lrp.liao@outlook.com

Cite this article: Yu C., Zeng Z.-l., Cai X., Chen Z.-h., & Liao R.-p. (2024). Adsorption-desorption of lead by polycarboxylate-coated bentonite. *Clays and Clay Minerals* 72, e4, 1–12. <https://doi.org/10.1017/cmn.2024.2>

clay minerals (Uddin, 2017) as primary adsorbents for heavy metal removal. Among these, clay minerals, especially bentonite, outperform other commercial adsorbents due to their superior adsorption performance, cost-effectiveness, and widespread availability. Bentonite, primarily composed of montmorillonite, boasts an exceptionally high specific surface area and a lamellar structure (Yu *et al.*, 2019a). The surplus surface negative charge of montmorillonite allows bentonite to adsorb heavy metals through both surface adsorption and ion exchange concurrently. This property has led to its extensive use in various adsorption scenarios and permeable reactive barrier materials (Yu *et al.*, 2021). However, natural bentonite is limited in industrial applications for its low quality and easy desorption (Han *et al.*, 2019). Consequently, the modification of bentonite to enhance its adsorption capacity presents a promising avenue with broad application prospects.

Various techniques have been explored to modify bentonite, including acid activation (Malamis and Katsou, 2013; Fazlali *et al.*, 2019), calcination (Aytas *et al.*, 2009), pillared (Manohar *et al.*, 2005; Tomul, 2012), surfactant treatment (Ghiaci *et al.*, 2007; Díaz-Nava *et al.*, 2012; Xie *et al.*, 2023b), activator loading (Cai *et al.*, 2019; Shao *et al.*, 2018; Yu *et al.*, 2019b; Li *et al.*, 2020; Yu *et al.*, 2020) and polymer modification (Souza and Nascimento, 2008; Kotal and Bhowmick, 2015; Wang *et al.*, 2016; Xie *et al.*, 2023a). Acid activation can unclog pore channels, increase the specific surface area, and enhance the adsorption activity of metal ions by dissolving natural cementing impurities in the bentonite, leading to hydrogen ion substitution at the adsorption site. Calcination, while increasing the specific surface area by gasifying strongly bound water, requires high temperature and energy consumption. Pillaring, although it extends the distance between bentonite layers, destroys the free property between layers, making montmorillonite's structure similar to zeolite and reducing swelling properties. Surfactant treatment follows the cation exchange principle to increase bentonite's organic adsorption capacity. Yet, the difficulty in replacing the surfactants introduced with metal cations reduces its exchange adsorption capacity for heavy metals. Polymer-modified bentonite can change the specific surface area, pore volume, and functional group content of soil particles (such as $-\text{NH}_2$, $-\text{COOH}$, and $-\text{OH}$) due to its polymer structure characteristics. The organic chains introduced are also expected to remove heavy metals and organic pollutants simultaneously (Han *et al.*, 2019), which has become a popular direction for bentonite modification. However, there are few studies on the co-adsorption mechanism of polymers and clays, especially desorption. This is very important for understanding the adsorption mechanism of heavy metals and the recycling of adsorbents.

In addition, most heavy metals exist as positively charged ions, prompting a common strategy to enhance bentonite's adsorption capacity through the introduction of negative charge or polar functionalities. However, challenges arise due to disparities in hydration and swelling, hindering the formation of stable composite materials between polymers and clay minerals. In this study, sodium polyacrylate, recognized for its high efficiency and abundant negative charges, was grafted onto bentonite using an organosilane coupling agent. This nanocomposite synthesis aimed to investigate the adsorption and desorption characteristics of lead ions, representing cationic metal pollutants, on the polycarboxylate-grafted bentonite (SAPAS-Bentonite). The results provide valuable insights into the potential applications and adsorption mechanisms of this sodium polyacrylate modified clay, paving the way for future advancements in this field.

Materials and Methods

Materials and reagents

The raw bentonite used in this study was sourced from Yixing Jintai Geotechnical Materials Co., Ltd, located in Jiangsu, China. Before utilization, the bentonite underwent a purification process involving sieving through a 200-mesh (75 μm) sieve and subsequent drying in an oven at 105°C for 48 h. The purified bentonite was stored in a polypropylene container within a desiccator. Mineral analysis indicated that the raw bentonite consists of montmorillonite (45%), quartz (24%), heulandite (15%), and calcite (15%), with a cation exchange capacity (CEC) of 66.08 cmol kg^{-1} . All chemicals used in the experiments were procured from Shanghai Aladdin Biochemical Technology Co., Ltd, and met analytical purity standards. Solutions for the experiments were prepared using deionized water.

Methods

Synthesis of SAPAS-Bentonite

SAPAS-Bentonite was synthesized through solution polymerization (Yu *et al.*, 2019a), employing raw bentonite, triethoxyvinylsilane, acrylic acid, and other auxiliary materials in the dosages depicted in Table 1. The synthesis consisted of two steps (Fig. 1): (1) the grafting of alkenylsilanol groups onto mineral surfaces in bentonite; and (2) the double bond polymerization of acrylic acid with alkene groups. Initially, triethoxyvinylsilane underwent hydrolysis in deionized water, followed by the addition of bentonite to form a slurry. This slurry was stirred continuously at 85°C for 60 min,

Table 1. The raw materials and ratio of SAPAS-Bentonite

Raw materials	Chemical formula	CSA	Dosage (g or ml)
Triethoxyvinylsilane (l)	$\text{CH}_2=\text{CHSi}(\text{OC}_2\text{H}_5)_3$	78–08–0	2.00
Acrylic acid (l)	$\text{CH}_2=\text{CHCOOH}$	79–10–7	6.00
N,N'-Methylenebis (acrylamide) (s)	$\text{CH}_2(\text{NHCOCH}=\text{CH}_2)_2$	110–26–9	0.50
Potassium persulfate (s)	$\text{K}_2\text{S}_2\text{O}_8$	7727–21–1	0.30
Sodium hydroxide (s)	NaOH	1310–73–2	3.34*
Deionized water (l)	H_2O	—	250.00
Raw bentonite (s)	—	—	20.00

*The amount of NaOH used here is approximate.

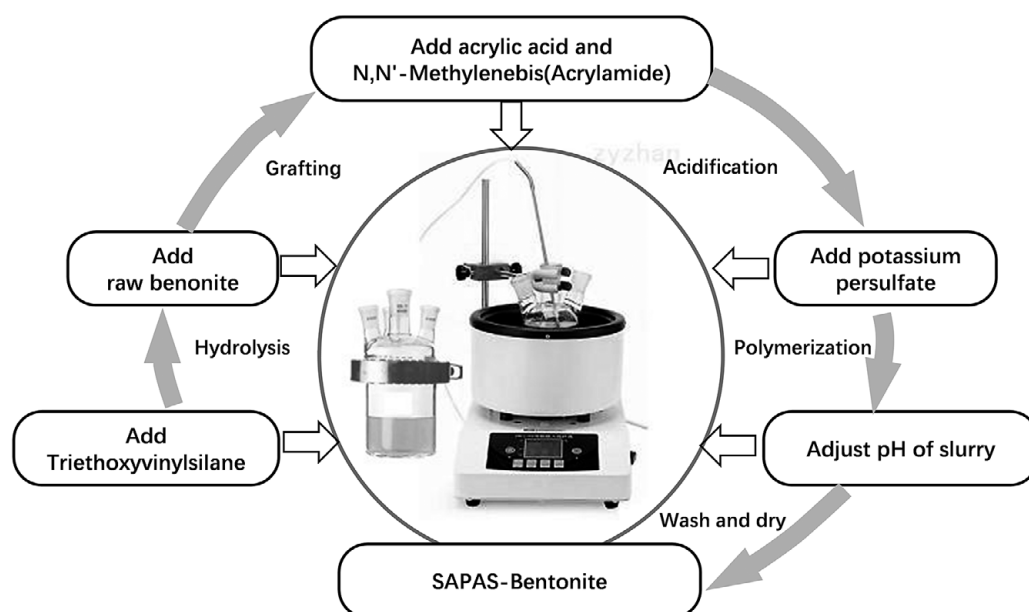


Figure 1. Flowchart of preparation of SAPAS-Bentonite.

Table 2. Batch adsorption and experiments parameters

Sorbents	t (min)	pH	c_i (mg l ⁻¹)	T (°C)
Raw bentonite	720	4	800–1900	25
or				
SAPAS–Bentonite	720	2–6	1000	25
	720	4	1000	7–65
	6–1440	4	1000	25

Table 3. Batch desorption and experiments parameters

Amount of lead ions adsorbed	t (min)	pH	T (°C)
95.4 mg g ⁻¹ for raw bentonite	720	4	25
or			
106.3 mg g ⁻¹ for SAPAS–Bentonite	720	2–6	25
	720	4	7–65
	6–1440	4	25

facilitating the completion of grafting. Subsequently, *N,N'*-methylenebisacrylamide, and acrylic acid were introduced, followed by the addition of potassium persulfate to initiate polymerization after 30 min of stirring. Finally, the pH of the slurry was adjusted to 7 using sodium hydroxide, after which it was centrifuged, washed repeatedly, and dried at 105°C.

Batch adsorption and desorption experiments

Both adsorption and desorption tests were conducted in batches. In the adsorption batch, 0.1 g of bentonite was added to 15 mL centrifuge tubes containing 10 mL of lead ions solution at a pre-determined concentration. The contents were mixed gently for a specific time at a designated temperature. The desorption process followed a similar procedure, using lead-adsorbed bentonite and a desorption reagent instead of initial bentonite. The lead-adsorbed raw bentonite adsorbed 95.4 mg g⁻¹ of lead ions, while SAPAS-Bentonite adsorbed 106.3 mg g⁻¹. These adsorbed samples were dried, ground, and used for desorption experiments. For concentration-dependent desorption, the tubes were oven-dried after adsorption (without centrifugal separation), ground, and reused. Soil–water separation operations were carried out by centrifugation (5867×g using a Xiangyi H1850, Changsha, China) at 8000 r.p.m. for 3 min, excluding the acceleration phase. It is noteworthy that centrifugation time was included in dynamic timing analyses. The residual or dissociated metal ions before and after experiments were analyzed using a flame atomic absorption spectrophotometer (Shimadzu AA6880F, Kyoto, Japan). The effects of adsorbent initial concentration (c_i), pH value, experimental

temperature (T), and contact time (t) on the adsorption capacity were examined (Tables 2 and 3). pH was adjusted using 0.1 M and 0.01 M HCl or NaOH. Adsorption amounts were determined by comparing the concentration of lead ions before and after the adsorption or desorption process. Each experiment was conducted twice to ensure accuracy.

Theoretical approach

The per cent adsorption (%) of lead ions was calculated using:

$$\text{Adsorption}(\%) = \frac{c_i - c_e}{c_i} \times 100, \quad (1)$$

where c_i is the initial concentration of the lead ions solution (mg L⁻¹), and c_e is the equilibrium concentration of the lead ions solution (mg L⁻¹). Similarly, the adsorption capacity (q_e , mg g⁻¹) was calculated as:

$$q_e = \frac{(c_i - c_e)v}{10m_{\text{ads}}}, \quad (2)$$

where v is the volume of lead ions solution (mL) and m_{ads} is the mass of the adsorbent (g).

In this study, equilibrium experimental data for the adsorption of lead ions on the composite were analyzed using the Langmuir and Freundlich isotherm models to describe the adsorption data. The Langmuir model (Langmuir, 1918) is expressed as:

$$q_e = \frac{q_m b c_e}{1 + b c_e}. \quad (3)$$

The model can be expressed in a linear form as:

$$\frac{c_e}{q_e} = \frac{1}{bq_m} + \frac{c_e}{q_m}, \quad (4)$$

where q_m denotes the maximum adsorption capacity (mg g^{-1}), and b is the Langmuir adsorption equilibrium constant (L mg^{-1}), which is related to the heat of adsorption. This linear form proves useful for plotting and analyzing experimental data.

The expression of Freundlich model (Freundlich, 1907), an empirical equation describing adsorption to heterogeneous surface, is given as:

$$q_e = K_F c_e^n. \quad (5)$$

The model also can be expressed in the linear form as:

$$\log q_e = \log K_F + n \log c_e, \quad (6)$$

where F and n are the Freundlich coefficients; the former represents the adsorption capacity when the metal ion equilibrium concentration equals 1, and the latter represents the degree of dependence of the adsorption on the equilibrium concentration.

Kinetics for clay–metal interaction was adjusted in this study by applying the pseudo-first order kinetics and pseudo-second order kinetics equations (Ezzati, 2020). The two models are discrete and are expressed as:

$$\ln(q_e - q_t) = \ln(q_e) - k_1 t, \quad (7)$$

and

$$\frac{t}{q_t} = \frac{1}{k_2 q_e^2} + \frac{t}{q_e}, \quad (8)$$

where q_e and q_t are the values for the adsorbed amount per unit mass at equilibrium and at any given time t , and k_1 and k_2 are discrete and the pseudo-first order and pseudo-second order adsorption rate constants.

Characterizations analysis

X-ray diffraction (XRD) analysis was conducted using a Bruker D8 Advance X-ray diffractometer (Karlsruhe, Germany), with $\text{CuK}\alpha$ radiation ($\lambda = 1.5406 \text{ \AA}$) at a scanning rate of 8° min^{-1} in the 2θ range from 5 to 75° . Thermogravimetric analysis (TGA) was performed using Perkin Elmer TGA instrument (Diamond TG-DTA, Waltham, MA, USA) at a heating rate of $10^\circ\text{C min}^{-1}$ in an oxygen atmosphere. The microstructure of bentonites, post-adsorption at varying lead concentrations, was examined using scanning electron microscopy (SEM) with an FEI Nova NanoSEM 200 instrument (Hillsboro, OR, USA) at a magnification range of $5000\text{--}30,000\times$. The bentonite samples were evaluated according to the Chinese standard for bentonite (GB/T 20973-2020). Specifically, all exchangeable cations in the bentonite samples were replaced by

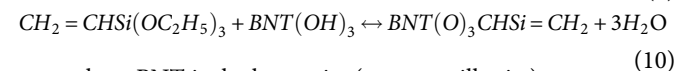
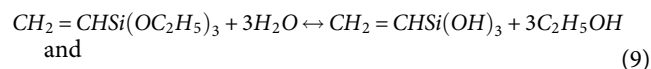
Ba^{2+} using a BaCl_2 solution to obtain pure Ba-bentonite. Subsequently, Ba-bentonite underwent a full exchange of Ba^{2+} to Mg^{2+} in a MgSO_4 solution, as Ba^{2+} is completely precipitated by SO_4^{2-} . Finally, the CEC value was determined by measuring the reduction of Mg^{2+} in the MgSO_4 solution.

Results and Discussion

Preparation of SAPAS-Bentonite

The modified substance of polycarboxylate graft-coated bentonite represents the mineral modification of montmorillonite, the primary active mineral. The crystal edges of montmorillonite are abundant in hydroxyl groups such as Si-OH and Al-OH . Consequently, the silanol groups, generated by organosilane hydrolysis, can readily dehydrate and condense with the original hydroxyl structure of montmorillonite. This process enables the growth of triethoxyvinylsilane on the mineral surface. According to several studies on silicone adhesives (Pape, 2011; Stewart *et al.*, 2013), silicon hydroxyl groups appear capable of achieving chemical bonding, even in the absence of hydroxyl structural clay mineral surfaces. To achieve a strong bond between sodium polyacrylate and bentonite, the preparation process of modified soil can be divided into two processes: the grafting of triethoxyvinylsilane and the polymerization of the acrylic root monomer. The chemical reaction principle in the preparation process is described below.

- (1) The graft reaction mechanism of bentonite is as follows:

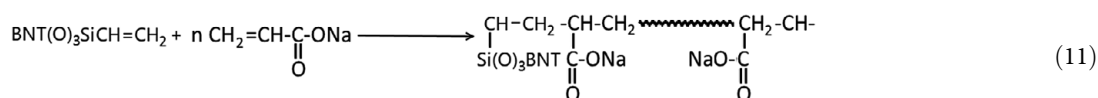


where BNT is the bentonite (montmorillonite) group.

- (2) The acidic environment, provided by acrylic acid, was conducive to silane hydrolysis and the dissolution of carbonate impurity minerals (calcite) in bentonite. This process unclogged the inner pores of clay particles. Finally, the excess acid was neutralized by NaOH to form sodium polyacrylate.
- (3) $\text{N,N}'$ -Methylenebisacrylamide was used as a crosslinking agent, which helps to form intersections in the polymerization process.
- (4) $\text{K}_2\text{S}_2\text{O}_8$ was used to trigger the reaction as an initiator.

The polymerization process occurs through a free radical reaction and involves chain initiation, chain growth, and end-of-chain termination:

- (1) The acrylic monomers are separated into a linear chain due to the effect of the initiator ($\text{K}_2\text{S}_2\text{O}_8$):



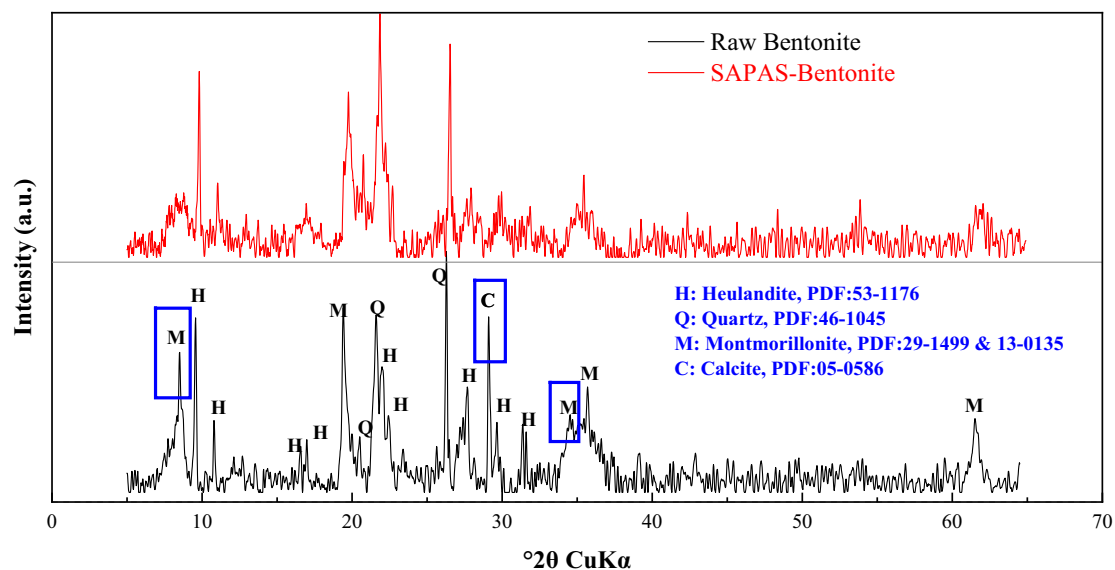


Figure 2. XRD patterns of raw bentonite and SAPAS-Bentonite.

adsorption percentage of SAPAS-Bentonite also reflects the contribution of sodium polyacrylate (Chen *et al.*, 2022). Similarly, SAPAS-Bentonite reached desorption equilibrium faster, at 62 min, compared with 360 min for raw bentonite. Both bentonites exhibited relatively low desorption, indicating stable adsorption. Given that SAPAS-Bentonite initially adsorbed more lead, the amount desorbed was also greater than that for raw bentonite.

Pseudo-first order (Fig. 5b) and pseudo-second order (Fig. 5c) equations were employed to fit the adsorption kinetics. Table 4 presents the linear correlation coefficients, pseudo-first order rate constant (k_1), pseudo-second order rate constant (k_2), and equilibrium capacity values. A comparison of the R^2 values indicates that the adsorption kinetics of all bentonites better fit the pseudo-second order model, whether in adsorption or desorption. This suggests that the adsorption or desorption rates depend mainly on the lead ion concentration and are proportional to its square. After all, adsorption and desorption are a pair of positive and negative reactions, and their relative rates determine the direction of the

adsorption reaction; the chemical mechanism remains the same. The faster adsorption rate of SAPAS-Bentonite can be attributed to differences in lead ion diffusion between the soil particles, facilitated by the water absorption and swelling of the polymer, which expands the diffusion channels. This diffusion control also applies to the desorption process.

Effect of temperature

In the adsorption reaction, the transformation of the adsorbate from a free state to a bound state is generally considered a process of entropy reduction. The spontaneity of the adsorption reaction also signifies the exothermic nature of the reaction process. However, for bentonites dominated by cation exchange adsorption (including SAPAS-Bentonite), the adsorption of lead ions is accompanied by the desorption of adsorbable exchange ions (such as sodium or calcium ions) at the original adsorption site. The entropy change in this process is not necessarily reduced and may even increase at times. Therefore, some adsorption processes involving bentonite can also be endothermic. Indeed, the adsorption thermodynamics of bentonite currently hold two main viewpoints: endothermic (Donat *et al.*, 2005; Karapinar and Donat, 2009) and exothermic (Xu, 2008; Taha *et al.*, 2016). Regardless of whether it is endothermic or exothermic, the value of the enthalpy change is small, indicating that the adsorption of bentonite is primarily a physical process. This suggests that the effect of temperature aligns consistently with the experimental phenomena observed in the initial months. This consistency underscores the reliability of the experimental results and the robustness of the physical processes involved in bentonite adsorption.

The effect of temperature on the adsorption and desorption of raw bentonite and SAPAS-Bentonite reveals that with an increase in temperature, the adsorption percentage of lead ions by raw bentonite and SAPAS-Bentonite decreases slightly, while the desorption amount increases (Fig. 6). This indicates that the adsorption of lead by bentonite is an exothermic process. In contrast to adsorption, desorption is an endothermic process, wherein the influence of temperature on lead ions in desorption is lower than that in adsorption. When the temperature rises from 10 to 50°C, the desorption rate of adsorbed lead in the modified

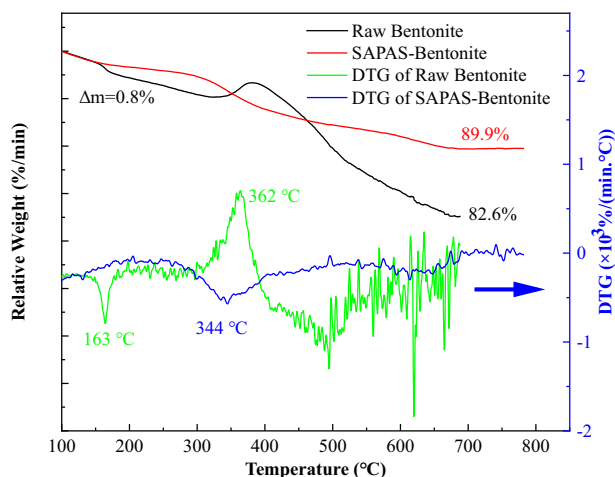


Figure 3. The TGA/TG curves of raw bentonite and SAPAS-Bentonite.

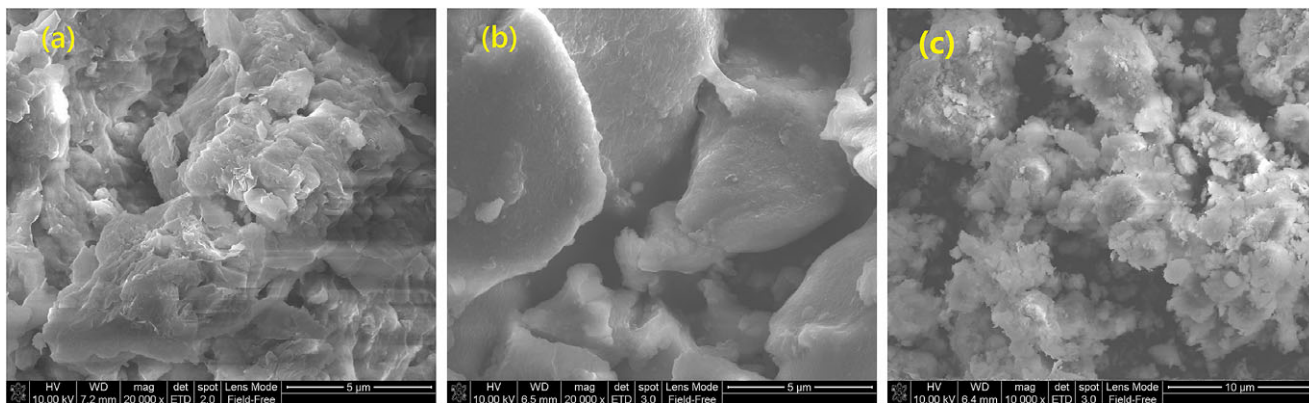


Figure 4. The SEM images of the material; (a) raw bentonite; (b) sodium polyacrylate; (c) SAPAS-Bentonite.

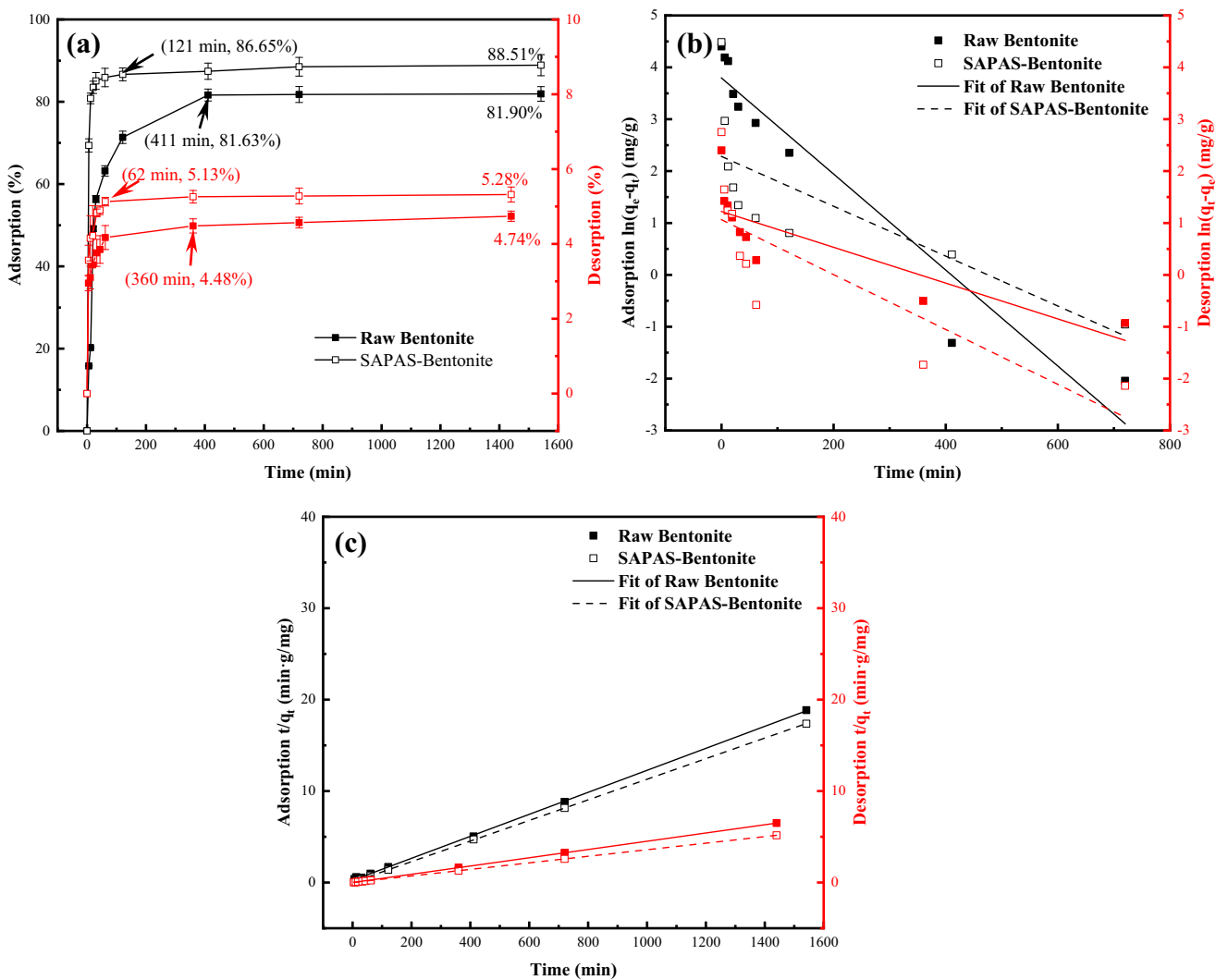


Figure 5. Effect of contact time on adsorption and desorption of lead ions on the raw bentonite and SAPAS-Bentonite: (a) the adsorption and desorption curve; (b) pseudo-first order kinetic model; (c) second-order kinetic model ($c_i=1000 \text{ mg L}^{-1}$, $\text{pH}=4$, $T=25^\circ\text{C}$).

Table 4. Values of parameters of pseudo-first order and pseudo-second order models for the adsorption of lead ions on raw bentonite and SAPAS-Bentonite

Bentonites	Pseudo-first order			Pseudo-second order		
	k_1	q_e (mg g ⁻¹)	R^2	k_2	q_e (mg g ⁻¹)	R^2
Raw bentonite (adsorption)	0.0093	44.48	0.0915	0.0006	83.33	0.9997
SAPAS-Bentonite (adsorption)	0.0048	9.80	0.5323	0.0043	90.91	0.9999
Raw bentonite (desorption)	0.0034	3.39	0.6496	-0.011	222.22	0.9999
SAPAS-Bentonite (desorption)	0.0053	2.90	0.6138	-0.02	277.78	0.9999

Table 5. The parameters for Langmuir and Freundlich isotherms

Bentonites	Langmuir			Freundlich		
	q_m (mg g ⁻¹)	b	R^2	K_f	n	R^2
Raw bentonite (adsorption)	112.36	1.1	0.997	281.84	0.242	0.726
SAPAS-Bentonite (adsorption)	165.73	0.60	0.974	288.40	0.300	0.806
Raw bentonite (desorption)	128.53	0.88	0.999	75.86	0.423	0.202
SAPAS-Bentonite (desorption)	179.21	0.34	0.995	89.13	0.454	0.306

bentonite is 1.23%, which is larger than that of the raw bentonite at 0.6%. This demonstrates that the modified bentonite possesses good adsorption stability and also reflects that the adsorbed ion of polyacrylate is more easily desorbed than that of bentonite.

Effect of initial pH

The results of the adsorption and desorption of lead ions on raw bentonite and SAPAS-Bentonite (Fig. 7) demonstrate that the adsorption and desorption percentage curves of the two bentonites are similar. The adsorption capacity of SAPAS-Bentonite was found to be much greater than that of raw bentonite, particularly at pH>2.5. The decrease in pH of the adsorption system has a noticeable inhibitory effect on the adsorption performance of both types of bentonites, and it is more pronounced in SAPAS-Bentonite. The desorption results reveal that the lead adsorbed by bentonite is stable

and the desorption amount is very small at solution pH>3. The decrease in pH results in the inhibition of lead adsorption and the promotion of desorption in bentonite, which is related to the competitive adsorption of H⁺. In the system, H⁺, as the competitive cation of lead ions, is bound to reduce the adsorption of lead ions when the total amount of exchangeable cation is fixed.

The competitive adsorption capacity of ions in bentonite depends mainly on the concentration, valence state, and ionic radius of ions (Chen *et al.*, 2012). When pH>3, the concentration of hydrogen ions is small enough not to constitute significant adsorption competition because the pH is the negative logarithm of the concentration of hydrogen ions. In addition, after bentonite adsorbs enough hydrogen ions, the originally negatively charged mineral surface will be positively charged, which further inhibits the exchange adsorption of positively charged lead ions. The carboxylic

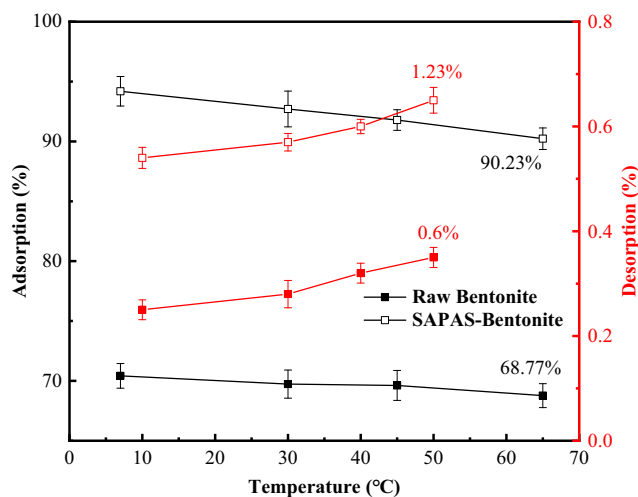
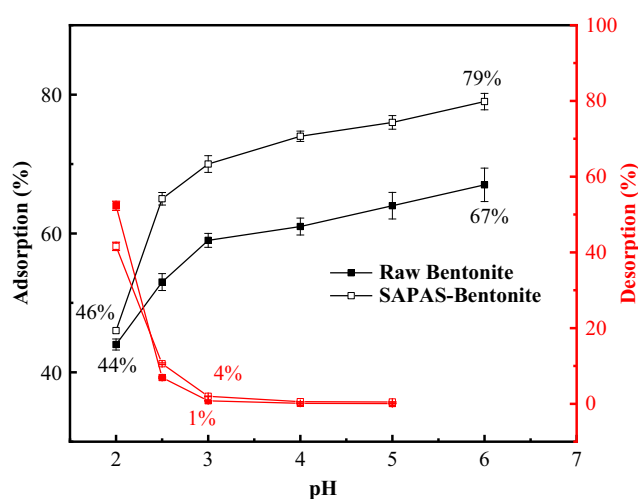
**Figure 6.** Effect of temperature on adsorption and desorption of lead ions on the raw bentonite and SAPAS-Bentonite ($c_i=1000$ mg L⁻¹, pH=4, $t=720$ min).**Figure 7.** Effect of pH on adsorption and desorption of lead ions on the raw bentonite and SAPAS-Bentonite ($c_i=1000$ mg L⁻¹, $t=720$ min, $T=25^\circ\text{C}$).

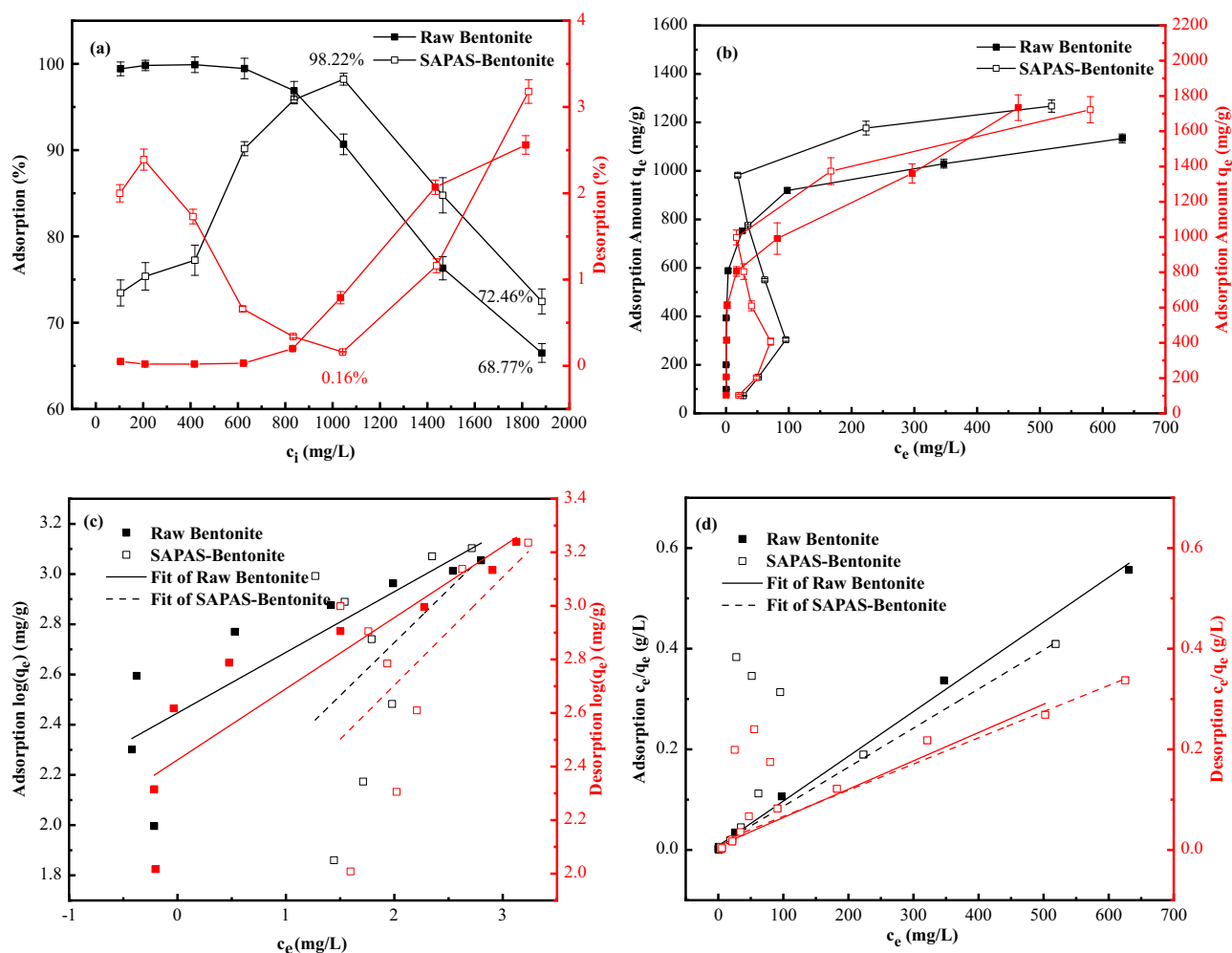
Table 6. The maximum adsorption capacity of lead ions by various adsorbents in literature

Adsorbent	q_m (cmol kg ⁻¹)	Reference
Fe, Mg (hydr)oxides coatings bentonite	46.3	(Randelović et al., 2012)
GMZ bentonite	47.9	(Wang et al., 2009)
MX-80 bentonite	33.1	(Xu, 2008)
Na-bentonite	23.1	(Yang et al., 2010)
ZnO-montmorillonite Nanocomposite	42.7	(Sani et al., 2017)
Organo-montmorillonites	30.5	(Liu et al., 2018)
MCM-41 synthesized montmorillonite	47.6	(Du et al., 2011)
MCM-41 synthesized kaolinite	35.4	(Du et al., 2011)
Sodium polyacrylate bentonite	72.89	(Chen et al., 2020)
Raw Bentonite	54.23	Present study
SAPAS-Bentonite	79.99	Present study

acid group ($-\text{COO}^-$) in SAPAS-Bentonite is a weak acid group, making it prone to binding hydrogen ions and rapidly reducing the negative charge on SAPAS-Bentonite. As a result, SAPAS-Bentonite is more sensitive to pH than raw bentonite.

Effect of initial concentrations of lead ions and isotherms models

The isothermal adsorption result serves as a key characterization of the pore properties of the adsorbent and the binding mode of the adsorbate. The maximum adsorption capacity of SAPAS-Bentonite for lead ions surpasses that of raw bentonite, and significant differences exist in the response of the two bentonites to the concentration of lead ions (Fig. 8). In terms of the adsorption curve, raw bentonite almost completely adsorbed lead ions at low concentrations ($c_i < 600 \text{ mg L}^{-1}$), while SAPAS-Bentonite could not. This phenomenon suggests that minerals such as montmorillonite and heulandite phases in SAPAS-Bentonite are indeed protected by sodium polyacrylate. The adsorption characteristics displayed at low concentrations indicate that the polymer is acting while the minerals in the soil particles do not seem to be exposed to lead ions because SAPAS-Bentonite actually possess full adsorption potential (Fig. 8a). This structural feature also causes the adsorption potential of clay minerals to be released and the adsorption rate to rise rapidly when the initial lead concentration increases and the sodium polyacrylate protection fails gradually. The failure of mineral

**Figure 8.** Isothermal adsorption/desorption equilibrium results of the raw bentonite and SAPAS-Bentonite. (a) Percentage of lead ions adsorbed; (b) the amount of lead ions adsorbed; (c) Freundlich isotherm; (d) Langmuir isotherm ($t=720 \text{ min}$, $\text{pH}=4$, $T=25^\circ\text{C}$).

protection in SAPAS-Bentonite is related to the increase in initial lead concentration and the gradual shrinkage of expanded sodium polyacrylate, leading to the opening of pores. SAPAS-Bentonite combines the adsorption properties of sodium polyacrylate and bentonite (Chen *et al.*, 2022), and successively works to display an S-shaped isothermal adsorption curve (Fig. 8b). The first half of the adsorption, led by sodium acrylate, is a typical capillary coacervated adsorption due to the variable structure of the sodium polyacrylate (Chen *et al.*, 2020). The second half is similar to the raw material bentonite, exhibiting a single-layer adsorption characteristic.

The characteristics of the desorption and adsorption curves of the two bentonites for lead are highly symmetric, as mentioned above. The comparison of adsorption capacity and desorption capacity at the same equilibrium concentration shows that the adsorption capacity is greater than the desorption capacity. This implies that some of the remaining lead ions cannot be completely desorbed. This phenomenon is probably caused by the pore structure of bentonite. In particular, the packaging protection of sodium polyacrylate prevents the lead ions adsorbed inside SAPAS-Bentonite particles from desorption, resulting in a higher retention rate of SAPAS-Bentonite than that of raw material bentonite.

The Langmuir and Freundlich models were employed to fit the adsorption and desorption data as a function of the linear form of the model (see Eqns (4) and (6)). The comparison of the fitting results of the two models (Table 5) reveals that the Langmuir isotherm model is more suitable for experimental data than the Freundlich model. SAPAS-Bentonite has two effective adsorption components, sodium polyacrylate and bentonite, and sodium polyacrylate has a 'protective' effect on bentonite at low concentrations ($c_1 < 1000 \text{ mg L}^{-1}$). It can be considered as a two-stage adsorption, as described above. When the adsorption of these two phases reaches saturation adsorption capacity, the Langmuir isotherm model fits well for SAPAS-Bentonite. The maximum adsorption capacity of SAPAS-Bentonite was 165.73 mg g^{-1} , which was much higher than that of the raw bentonite (112.36 mg g^{-1}) according to the Langmuir isotherm model. It indicates that the modification process can significantly improve the adsorption capacity of bentonite to heavy metal ions. The maximum adsorption capacity calculated by desorption is greater than that calculated by adsorption. The retention of raw bentonite is $\sim 16.17 \text{ mg g}^{-1}$ (14% adsorption capacity), and that of SAPAS-Bentonite is 13.48 mg g^{-1} (8.4% adsorption capacity). By comparing the maximum adsorption capacity of lead ions with other adsorbents in literature, it can be found that the modification method and SAPAS-Bentonite in this study have excellent adsorption capacity of lead ions (Table 6).

Conclusions

Based on the discussion of the results, the following conclusions can be drawn:

- Triethoxyvinylsilane served as a grafting agent, facilitating the connection between montmorillonite and sodium polyacrylate. This interaction led to the formation of a stable chemical bond between the polymer and the clay mineral. The modified bentonite retained its layered structure but acquired a protective film of sodium polyacrylate. This outer layer of polymer acted as a 'protective' shield for the inner bentonite particles, playing a crucial role in fortifying the clay minerals.
- The adsorption and desorption of lead ions by raw bentonite or SAPAS-Bentonite are primarily affected by pH and initial

concentration, with the effect of temperature being negligible. Under the same conditions, the trend of adsorption and desorption is similar, but the adsorption equilibrium is not consistent. Lead ions adsorbed by bentonite and SAPAS-Bentonite are not easily desorbed. Desorption capabilities of raw bentonite and SAPAS-Bentonite are low in conventional natural water environments with $\text{pH} > 3$. In addition, $\sim 14\%$ of heavy metals adsorbed by bentonite are retained and challenging to desorb, while that of polycarboxylate is reversible. The isothermal adsorption pattern of raw bentonite is close to the Langmuir model, while SAPAS-Bentonite presents an S-shaped composite isothermal adsorption curve.

- Carboxylic groups exhibit distinct ion adsorption features compared with ion exchange in bentonite, effectively increasing its heavy metal adsorption capacity, with a greater priority than that of bentonite. The presence of polycarboxylate reduces the initial adsorption of heavy metals by bentonite until polycarboxylate saturation arises. The incorporation of 30% acrylic acid (relative to the quantity of raw bentonite) enhances the adsorption capacity for heavy metal lead by 47.5%, as indicated by the Langmuir isotherm model.

In summary, the adsorption and desorption characteristics of bentonite and SAPAS-Bentonite as adsorbents for lead ions were studied thoroughly here, providing a reliable evaluation and reference for the use and reuse of the two clays in heavy metals adsorption. In particular, the modification technology of polycarboxylate-grafted bentonite was proposed, effectively improving the adsorption capacity of heavy metals, and revealing the modification mechanism and special characteristics of ion adsorption. The SAPAS-Bentonite developed shows a broad application prospect in the treatment of heavy metal-contaminated soil and water.

Author contribution. Chuang Yu: Methodology; Writing - Review & Editing; Funding acquisition; Project administration; Supervision; Zhi-lei Zeng: Investigation; Visualization; Writing - Original Draft; Xiaoqing Cai: Resources; Formal analysis; Zhi-hao Chen: Formal analysis; Rao-ping Liao: Conceptualization; Investigation; Data Curation; Writing - Review & Editing.

Acknowledgements. none.

Financial support. This work was supported by the National Natural Science Foundation of China (grant number: 52178352), Zhejiang Provincial Natural Science Foundation (grant number: Ltgs24e080004), and the Plan Project of Science and Technology of Wenzhou (grant number: ZS2021001).

Competing interest. The authors declare that they have no known competing financial interests or personal relationships that could have appeared to influence the work reported in this paper.

Data availability statement. The datasets used and analyzed during the current study are available from the corresponding author on reasonable request.

References

- Abdullah, N., Yusof, N., Lau, W. J., Jaafar, J., & Ismail, A. F. (2019). Recent trends of heavy metal removal from water/wastewater by membrane technologies. *Journal of Industrial and Engineering Chemistry*, 76, 17–38. <https://doi.org/10.1016/j.jiec.2019.03.029>
- Atteia, O., Del Campo Estrada, E., & Bertin, H. (2013). Soil flushing: a review of the origin of efficiency variability. *Reviews in Environmental Science and Bio/Technology*, 12, 379–389. <https://doi.org/10.1007/s11157-013-9316-0>

- Aytas, S., Yurtlu, M., & Donat, R. (2009). Adsorption characteristic of U(VI) ion onto thermally activated bentonite. *Journal of Hazardous Materials*, 172, 667–674. <https://doi.org/10.1016/j.jhazmat.2009.07.049>
- Bai, J., & Zhao, X. (2020). Ecological and human health risks of heavy metals in shooting range soils: a meta assessment from China. *Toxics*, 8, 32. <https://doi.org/10.3390/toxics8020032>
- Cai, X., Yu, X., Yu, X., Wu, Z., Li, S., & Yu, C. (2019). Synthesis of illite/iron nanoparticles and their application as an adsorbent of lead ions. *Environmental Science and Pollution Research*, 26, 29449–29459. <https://doi.org/10.1007/s11356-019-06136-4>
- Chai, W. S., Cheun, J. Y., Kumar, P. S., Mubashir, M., Majeed, Z., Banat, F., Ho, S.-H., & Show, P. L. (2021). A review on conventional and novel materials towards heavy metal adsorption in wastewater treatment application. *Journal of Cleaner Production*, 296, 126589. <https://doi.org/10.1016/j.jclepro.2021.126589>
- Chen, Y., Liao, R., Yu, C., & Yu, X. (2020). Sorption of Pb(II) on sodium polyacrylate modified bentonite. *Advanced Powder Technology*, 31, 3274–3286. <https://doi.org/10.1016/j.apt.2020.06.011>
- Chen, Y., Zhu, B., Wu, D., Wang, Q., Yang, Y., Ye, W., & Guo, J. (2012). Eu(III) adsorption using di(2-thylhexyl) phosphoric acid-immobilized magnetic GMZ bentonite. *Chemical Engineering Journal*, 181–182, 387–396. <https://doi.org/10.1016/j.cej.2011.11.100>
- Chen, Z., Yu, C., Dong, H., Cai, X., Liao, R., Zeng, Z., & Ye, C. (2022). Sorption-desorption characteristics and internal mechanism of lead ions on polycarboxylic ion exchange resin. *Journal of Polymer Research*, 29, 512. <https://doi.org/10.1007/s10965-022-03360-4>
- Chipasa, K. B. (2003). Accumulation and fate of selected heavy metals in a biological wastewater treatment system. *Waste Management*, 23, 135–143. [https://doi.org/10.1016/S0956-053X\(02\)00065-X](https://doi.org/10.1016/S0956-053X(02)00065-X)
- Dąbrowski, A., Hubicki, Z., Podkościelny, P., & Robens, E. (2004). Selective removal of the heavy metal ions from waters and industrial wastewaters by ion-exchange method. *Chemosphere*, 56, 91–106. <https://doi.org/10.1016/j.chemosphere.2004.03.006>
- Deliyanni, E. A., Kyzas, G. Z., Triantafyllidis, K. S., & Matis, K. A. (2015). Activated carbons for the removal of heavy metal ions: a systematic review of recent literature focused on lead and arsenic ions. *Open Chemistry*, 13, 000010151520150087. <https://doi.org/10.1515/chem-2015-0087>
- Díaz-Nava, M. C., Olguín, M. T., & Solache-Ríos, M. (2012). Adsorption of phenol onto surfactants modified bentonite. *Journal of Inclusion Phenomena and Macrocyclic Chemistry*, 74, 67–75. <https://doi.org/10.1007/s10847-011-0084-6>
- Donat, R., Akdogan, A., Erdem, E., & Cetisli, H. (2005). Thermodynamics of Pb²⁺ and Ni²⁺ adsorption onto natural bentonite from aqueous solutions. *Journal of Colloid and Interface Science*, 286, 43–52. <https://doi.org/10.1016/j.jcis.2005.01.045>
- Du, E., Yu, S., Zuo, L., Zhang, J., Huang, X., & Wang, Y. (2011). Pb(II) sorption on molecular sieve analogues of MCM-41 synthesized from kaolinite and montmorillonite. *Applied Clay Science*, 51, 94–101. <https://doi.org/10.1016/j.clay.2010.11.009>
- Ezzati, R. (2020). Derivation of pseudo-first-order, pseudo-second-order and modified pseudo-first-order rate equations from Langmuir and Freundlich isotherms for adsorption. *Chemical Engineering Journal*, 392, 123705. <https://doi.org/10.1016/j.cej.2019.123705>
- Faisal, A. A. H., Sulaymon, A. H., & Khalief, Q. M. (2018). A review of permeable reactive barrier as passive sustainable technology for groundwater remediation. *International Journal of Environmental Science and Technology*, 15, 1123–1138. <https://doi.org/10.1007/s13762-017-1466-0>
- Farrell, M., & Jones, D. L. (2009). Critical evaluation of municipal solid waste composting and potential compost markets. *Bioresource Technology*, 100, 4301–4310. <https://doi.org/10.1016/j.biortech.2009.04.029>
- Fazlali, F., Mahjoub, A. R., & Aghayan, H. (2019). Adsorption of toxic heavy metals on organofunctionalized acid activated exfoliated bentonite clay for wastewater treatment goals. *Desalination and Water Treatment*, 152, 338–350. <https://doi.org/10.5004/dwt.2019.23996>
- Freundlich, H. (1907). Über die adsorption in lösungen. *Zeitschrift für Physikalische Chemie*, 57U, 385–470. <https://doi.org/10.1515/zpch-1907-5723>
- Ghiaci, M., Kalbasi, R. J., & Abbaspour, A. (2007). Adsorption isotherms of non-ionic surfactants on Na-bentonite (Iran) and evaluation of thermodynamic parameters. *Colloids and Surfaces A: Physicochemical and Engineering Aspects*, 297, 105–113. <https://doi.org/10.1016/j.colsurfa.2006.10.032>
- Han, H., Rafiq, M. K., Zhou, T., Xu, R., Mašek, O., & Li, X. (2019). A critical review of clay-based composites with enhanced adsorption performance for metal and organic pollutants. *Journal of Hazardous Materials*, 369, 780–796. <https://doi.org/10.1016/j.jhazmat.2019.02.003>
- Järup, L. (2003). Hazards of heavy metal contamination. *British Medical Bulletin*, 68, 167–182. <https://doi.org/10.1093/bmb/ldg032>
- Ji, K., Kim, J., Lee, M., Park, S., Kwon, H.-J., Cheong, H.-K., Jang, J.-Y., Kim, D.-S., Yu, S., Kim, Y.-W., Lee, K.-Y., Yang, S.-O., Jhung, I. J., Yang, W.-H., Paek, D.-H., Hong, Y.-C., & Choi, K. (2013). Assessment of exposure to heavy metals and health risks among residents near abandoned metal mines in Goseong, Korea. *Environmental Pollution*, 178, 322–328. <https://doi.org/10.1016/j.envpol.2013.03.031>
- Karapinar, N., & Donat, R. (2009). Adsorption behaviour of Cu²⁺ and Cd²⁺ onto natural bentonite. *Desalination*, 249, 123–129. <https://doi.org/10.1016/j.desal.2008.12.046>
- Kharazi, A., Leili, M., Khazaei, M., Alikhani, M. Y., & Shokoohi, R. (2021). Human health risk assessment of heavy metals in agricultural soil and food crops in Hamadan, Iran. *Journal of Food Composition and Analysis*, 100, 103890. <https://doi.org/10.1016/j.jfca.2021.103890>
- Kotal, M., & Bhowmick, A. K. (2015). Polymer nanocomposites from modified clays: recent advances and challenges. *Progress in Polymer Science*, 51, 127–187. <https://doi.org/10.1016/j.progpolymsci.2015.10.001>
- Kurniawan, T. A., Chan, G. Y. S., Lo, W.-H., & Babel, S. (2006). Physico-chemical treatment techniques for wastewater laden with heavy metals. *Chemical Engineering Journal*, 118, 83–98. <https://doi.org/10.1016/j.cej.2006.01.015>
- Langmuir, I. (1918). The adsorption of gases on plane surfaces of glass, mica and platinum. *Journal of the American Chemical Society*, 40, 1361–1403. <https://doi.org/10.1021/ja02242a004>
- Lee, D., & Char, K. (2002). Thermal degradation behavior of polyaniline in polyaniline/Na⁺-montmorillonite nanocomposites. *Polymer Degradation and Stability*, 75, 555–560. [https://doi.org/10.1016/S0141-3910\(01\)00259-2](https://doi.org/10.1016/S0141-3910(01)00259-2)
- Li, S.-Q., Yu, C., Wu, Z.-X., Cai, X.-Q., & Zha, F.-S. (2020). Effect of kaolin particle size on the removal of Pb(II) from aqueous solutions by kaolin-supported nanoscale zero-valent iron. *Materials Research Express*, 7, 045002. <https://doi.org/10.1088/2053-1591/ab83a3>
- Liu, C., Wu, P., Tran, L., Zhu, N., & Dang, Z. (2018). Organo-montmorillonites for efficient and rapid water remediation: sequential and simultaneous adsorption of lead and bisphenol A. *Environmental Chemistry*, 15, 286. <https://doi.org/10.1071/EN18057>
- Malamis, S., & Katsou, E. (2013). A review on zinc and nickel adsorption on natural and modified zeolite, bentonite and vermiculite: examination of process parameters, kinetics and isotherms. *Journal of Hazardous Materials*, 252–253, 428–461. <https://doi.org/10.1016/j.jhazmat.2013.03.024>
- Manohar, D. M., Noeline, B. F., & Anirudhan, T. S. (2005). Removal of vanadium(IV) from aqueous solutions by adsorption process with aluminum-pillared bentonite. *Industrial & Engineering Chemistry Research*, 44, 6676–6684. <https://doi.org/10.1021/ie0490841>
- Pape, P. G. (2011). Adhesion promoters: silane coupling agents. In M. Kutz (ed), *Applied Plastics Engineering Handbook* (pp. 503–517). William Andrew Publishing. <https://doi.org/10.1016/B978-1-4377-3514-7.10029-7>
- Randelović, M., Purenović, M., Zarubica, A., Purenović, J., Matović, B., & Momčilović, M. (2012). Synthesis of composite by application of mixed Fe, Mg (hydr)oxides coatings onto bentonite – a use for the removal of Pb(II) from water. *Journal of Hazardous Materials*, 199–200, 367–374. <https://doi.org/10.1016/j.jhazmat.2011.11.025>
- Sani, H. A., Ahmad, M. B., Hussein, M. Z., Ibrahim, N. A., Musa, A., & Saleh, T. A. (2017). Nanocomposite of ZnO with montmorillonite for removal of lead and copper ions from aqueous solutions. *Process Safety and Environmental Protection*, 109, 97–105. <https://doi.org/10.1016/j.psep.2017.03.024>
- Shao, J., Yu, X., Zhou, M., Cai, X., & Yu, C. (2018). Nanoscale zero-valent iron decorated on bentonite/graphene oxide for removal of copper ions from aqueous solution. *Materials*, 11, 945. <https://doi.org/10.3390/ma11060945>
- Souza, C. E. C., & Nascimento, R. S. V. (2008). Adsorption behavior of cationic polymers on bentonite. *Journal of Thermal Analysis and Calorimetry*, 94, 579–583. <https://doi.org/10.1007/s10973-007-8774-4>

- Stewart, A., Schlosser, B., & Douglas, E. P. (2013). Surface modification of cured cement pastes by silane coupling agents. *ACS Applied Materials & Interfaces*, 5, 1218–1225. <https://doi.org/10.1021/am301967v>
- Taha, A. A., Shreadah, M. A., Ahmed, A. M., & Heiba, H. F. (2016). Multi-component adsorption of Pb(II), Cd(II), and Ni(II) onto Egyptian Na-activated bentonite; equilibrium, kinetics, thermodynamics, and application for seawater desalination. *Journal of Environmental Chemical Engineering*, 4, 1166–1180. <https://doi.org/10.1016/j.jece.2016.01.025>
- Tan, X., Liu, Y., Zeng, G., Wang, X., Hu, X., Gu, Y., & Yang, Z. (2015). Application of biochar for the removal of pollutants from aqueous solutions. *Chemosphere*, 125, 70–85. <https://doi.org/10.1016/j.chemosphere.2014.12.058>
- Tomul, F. (2012). Adsorption and catalytic properties of Fe/Cr-pillared bentonites. *Chemical Engineering Journal*, 185–186, 380–390. <https://doi.org/10.1016/j.cej.2012.01.094>
- Uddin, M. K. (2017). A review on the adsorption of heavy metals by clay minerals, with special focus on the past decade. *Chemical Engineering Journal*, 308, 438–462. <https://doi.org/10.1016/j.cej.2016.09.029>
- Wang, L., Wang, Y., Ma, F., Tankpa, V., Bai, S., Guo, X., & Wang, X. (2019). Mechanisms and reutilization of modified biochar used for removal of heavy metals from wastewater: a review. *Science of the Total Environment*, 668, 1298–1309. <https://doi.org/10.1016/j.scitotenv.2019.03.011>
- Wang, S., Dong, Y., He, M., Chen, L., & Yu, X. (2009). Characterization of GMZ bentonite and its application in the adsorption of Pb(II) from aqueous solutions. *Applied Clay Science*, 43, 164–171. <https://doi.org/10.1016/j.clay.2008.07.028>
- Wang, Y., Chen, Y., Xie, H., Zhang, C., & Zhan, L. (2016). Lead adsorption and transport in loess-amended soil-bentonite cut-off wall. *Engineering Geology*, 215, 69–80. <https://doi.org/10.1016/j.enggeo.2016.11.002>
- Xie, H., Chen, C., Shi, Y., Zheng, Z., Chen, Y., & Yan, H. (2023a). Adsorption behavior of PAEs on Loess-HTMAC bentonite and its effects on the performance of cut-off walls. *Journal of Environmental Engineering*, 149, 04023016. [https://doi.org/10.1061/\(JOEEDU\)EEENG-7193](https://doi.org/10.1061/(JOEEDU)EEENG-7193)
- Xie, H., Wu, J., Yu, M., Yan, H., Masum, S., Cai, P., & Chen, Y. (2023b). Bisphenol a adsorption and transport in loess and cationic surfactant/hydrophilic polymer modified bentonite liners. *Journal of Environmental Management*, 336, 117604. <https://doi.org/10.1016/j.jenvman.2023.117604>
- Xu, D. (2008). Adsorption of Pb(II) from aqueous solution to MX-80 bentonite: effect of pH, ionic strength, foreign ions and temperature. *Applied Clay Science*, 41, 37–46. <https://doi.org/10.1016/j.clay.2007.09.004>
- Xu, D.-M., Fu, R.-B., Wang, J.-X., Shi, Y.-X., & Guo, X.-P. (2021). Chemical stabilization remediation for heavy metals in contaminated soils on the latest decade: available stabilizing materials and associated evaluation methods – a critical review. *Journal of Cleaner Production*, 321, 128730. <https://doi.org/10.1016/j.jclepro.2021.128730>
- Xu, Z., Zhang, Q., Li, X., & Huang, X. (2022). A critical review on chemical analysis of heavy metal complexes in water/wastewater and the mechanism of treatment methods. *Chemical Engineering Journal*, 429, 131688. <https://doi.org/10.1016/j.cej.2021.131688>
- Yang, S., Zhao, D., Zhang, H., Lu, S., Chen, L., & Yu, X. (2010). Impact of environmental conditions on the sorption behavior of Pb(II) in Na-bentonite suspensions. *Journal of Hazardous Materials*, 183, 632–640. <https://doi.org/10.1016/j.jhazmat.2010.07.072>
- Yu, C., Liao, R., Cai, X., & Yu, X. (2019a). Sodium polyacrylate modification method to improve the permeant performance of bentonite in chemical resistance. *Journal of Cleaner Production*, 213, 242–250. <https://doi.org/10.1016/j.jclepro.2018.12.179>
- Yu, C., Lv, J., Zhou, M., Cai, X., Zha, F., & Yu, X. (2019b). Remediation of heavy metal Pb(II) in aqueous solution using Kaolin-supported nano iron. *Materials Research Express*, 6, 1150h4. <https://doi.org/10.1088/2053-1591/ab525b>
- Yu, C., Shao, J., Sun, W., & Yu, X. (2020). Treatment of lead contaminated water using synthesized nano-iron supported with bentonite/graphene oxide. *Arabian Journal of Chemistry*, 13, 3474–3483. <https://doi.org/10.1016/j.arabj.2018.11.019>
- Yu, C., Yang, Y., Wu, Z., Jiang, J., Liao, R., & Deng, Y. (2021). Experimental study on the permeability and self-healing capacity of geosynthetic clay liners in heavy metal solutions. *Geotextiles and Geomembranes*, 49, 413–419. <https://doi.org/10.1016/j.geotextmem.2020.10.012>